International Conference on Space Optics—ICSO 2022

Dubrovnik, Croatia

3–7 October 2022

Edited by Kyriaki Minoglou, Nikos Karafolas, and Bruno Cugny,

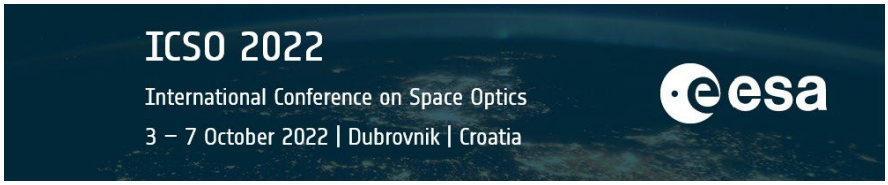

Design and validation of a new coding and synchronization layer for space optical communications

International Conference on Space Optics — ICSO 2022, edited by Kyriaki Minoglou, Nikos Karafolas, Bruno Cugny, Proc. of SPIE Vol. 12777, 127774S · © 2023 ESA and CNES · 0277-786X · doi: 10.1117/12.2690888

Design and validation of a new coding and synchronization layer for space optical communications

Géraldine Artaud*[a], Jean-Frederic Chouteau[b], Lyonel Barthe[b], Benjamin Gadat[b], Thomas Anfray[b], Sylvain Poulenard[b], Alain Dominique Thomas[c], Alain Quentel[c]
[a] CNES – 18, avenue Edouard Belin – 31 401 Toulouse Cedex 9 ; [b]Airbus D&S France - 31, Av. des Cosmonautes – 31 402 Toulouse Cedex 4– France ; [c] SDS – Safran Data Systems, 5 av. Des Andes, LES ULIS, France

ABSTRACT

The article presents a communication chain designed for space-earth optical data transmissions , and in particular the coding and synchronization layer including a new Forward Error Correction (FEC) based on LDPC codes combined with a flexible interleaver, a variable data rate scheme, and the framing for frame synchronization and in-band signaling. The communication chain is currently under validation in an end to end test bed in laboratory, and will be used for two in orbit demonstration missions in 2023 and 2024.

1. INTRODUCTION

Optical communication is a promising solution for earth-space data transfer with LEO and GEO satellites for earth observation data downlink and very high speed Internet delivery. It provides a much larger bandwidth (up to multi-gigabit per second), however dedicated communication chain need to be developed in order to protect the transmitted signal against the propagation channel impairments.

In this article we address the design of a cost-efficient and flexible modem technology for multi-gigabit optical communication downlinks. To tackle this challenge, we investigate a new flexible and high-performance coding and synchronization layer that takes into account hardware constraints of state-of-the art on-board and ground hardware data processing technologies. In particular, we introduce the code design of a new Forward Error Correction (FEC) based on LDPC codes combined with a flexible interleaver in order to tackle deep optical fading. It provides a competitive trade-off between coding performance and implementation complexity. We also present a variable data rate scheme based on spreading factors, and a robust and flexible framing structure that enables to change on-the-fly coding rate, interleaver duration, and spreading factor. Indeed, the available coding rates combined with spreading factors allows to adapt the useful data rate depending of the power variations on a LEO satellite optical downlinks link.

The performances of the proposed solution have been assessed in simulation against various propagation channel fading vectors. This led to its future adoption by CCSDS as one of the two new schemes of the optical communications coding and synchronization recommended standard CCSDS 142.0-B-1 [1]: O3K LDPC.

The simulation results will present the synchronization robustness, FEC performances in presence of a fading temporal series defined within the CCSDS framework.

The performances are currently confirmed in laboratory on an end to end optical bench running at 10Gbps, that includes representative satellite emitter, propagation emulator applying to the optical signal fading vector, optical front-end, and a modem that performs, in real-time and in non-coherent, time synchronization, frame synchronization, de-interleaving and soft LDPC decoding.

2. TRANSMISSION CHANNEL AND RECEIVER MODEL

The communication chain needs to cope with the optical transmission channel and the receiver type. The transmission channel is composed of the combination of the propagation channel (that includes the effects of the dynamics of the satellite and the atmosphere), and of the turbulence mitigation scheme. The receiver architecture has an impact on the overall performance, for example for a signal of modulation OOK, the receiver on ground can either be composed of an avalanche photodiode (APD) or a preamplified receiver. In the first case, if the collecting area of the APD is wide enough, the received power fluctuations caused by the turbulences only consist of scintillations, whereas when adaptive optics (AO) is used in a single mode fiber preamplified receiver, the received power fluctuations will also depends on the phase error residuals not corrected by the AO system.
The sensitivity, gain and dominant noise of the front-end receiver are also dependent of the type of receiver. They can be described in a receiver model.

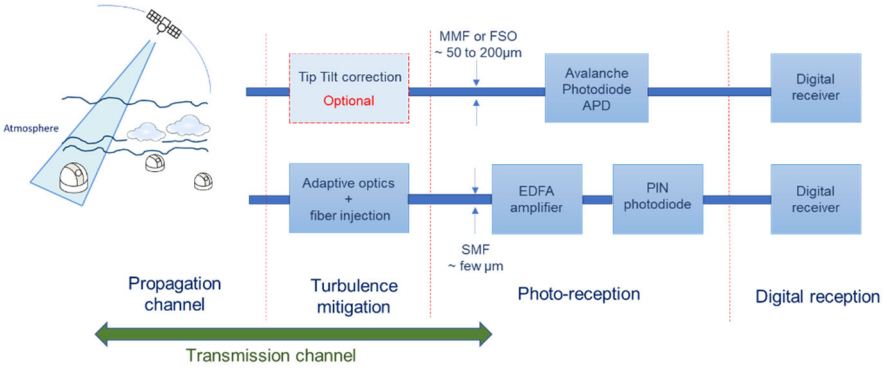

Figure 1: Example of 2 receiver architectures for modulation OOK.

2.1 Transmission channel

The transmission channel can be divided in two components. First a static components that do not vary quickly over time, which includes the power variation due to the distance between the emitter and the receiver, and the slow variations of the transmission through the atmosphere. For a LEO case, the static link loss vary with the elevation. The relative loss between the maximum received power at 90° and the loss at other elevations, can be calculated using the hypothesis of [2] and is shown in Figure 2 left. In a LEO link, the communication chain will have to cope with a wide range of power dynamics, and dedicated methods need to be implemented to adapt to the slow but large power variations, such as variable coding and variable data rate, as it will be shown in chapter 3.4.

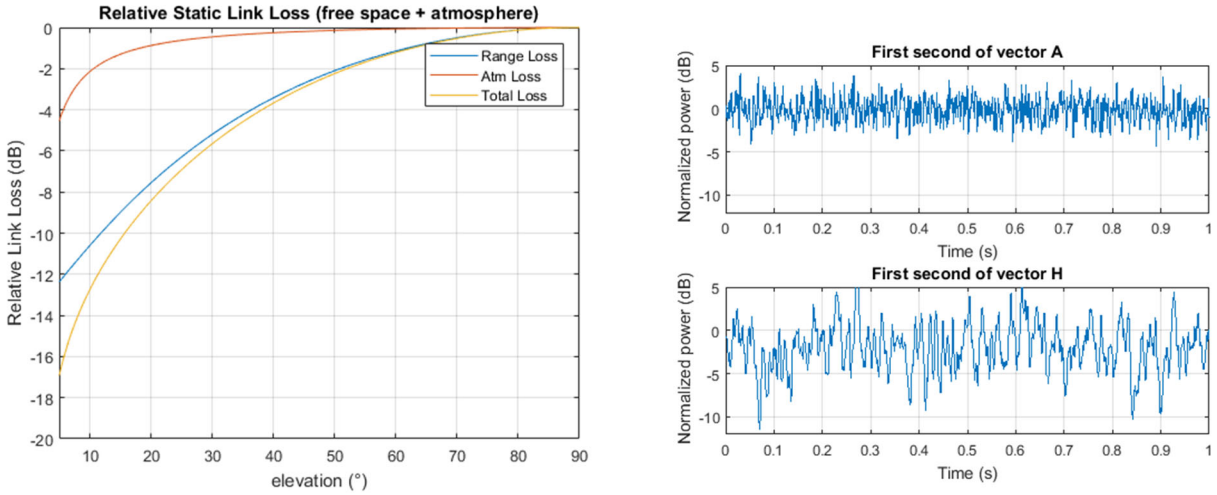

Figure 2: examples of transmission channels: static component (left), and dynamic component (right)

The second component of the transmission channel is dynamic, with the coherence time of power variations in the range of milliseconds. It includes the impairments caused by the atmospheric turbulences, and also the pointing jitter of the laser beam transmitted by the satellite. In the following part of the article we will consider a receiver architecture based on APD, for which the atmospheric turbulences are limited to scintillations. And more specifically we will use the power vectors A and H defined by DLR for the CCSDS standardization of coding and synchronization layer for LEO to ground optical link scenarios [3] [4]. These vectors were used to assess the proposed communication chain performances. Vector A corresponds to a favorable case with moderate scintillations, and H to a worst case with high scintillations corresponding to a transmission at about 5° elevation and pointing jitter. The first second of the 100 seconds fading vectors are plotted in Figure 2 right. In order to cope with the long fading, the error correcting codes are complemented by the use of long interleavers as it will be shown in chapter 3.2

2.2 Receiver model

In addition to the transmission channel, it is also needed to define a receiver model in order to properly test the communication chain performance. In this article we will not address the model of preamplified receiver, but rather focus on the APD receiver. A receiver noise model has been defined within the CCSDS SLS-OPT group [6] based on previous work of DLR [5] The model is recall hereafter for the case of interest: OOK data transmission at 10 Gbps:

The APD Receiver model defines for the received 0 and 1 the distribution of the noise. The noise of the received 0 is Gaussian thermal noise with zero mean and the noise on the received 1 is a combination of thermal noise and shot noise:

$y = N(\mu_i, \sigma_i^2), i = 0$ or 1, where $N(\mu_i,\ \sigma_i^2)$ is a Gaussian random variable with mean μ_i and variance σ_i^2, and

$$\mu_0 = 0 \qquad \mu_1 = \rho n_s$$
$$\sigma_0^2 = \frac{T_s \sigma_t^2}{2q^2M^2} \qquad \sigma_1^2 = \sigma_0^2 + F\rho n_s$$

where n_s is the average number of received photons per signal slot, with no fading, $\rho = 1$ and with fading, ρ values can be taken from a power vector time series. $T_s = 0.1$ ns is the symbol duration, i.e., channel rates of $R = 10\ Gbps$, $q = 1.602 \times 10^{-19}$ is the electron charge (C) , and the model assumes bandwidth $B = 1/(2T_s)$

The APD parameters are given by:

Parameter	symbol	CCSDS	Custom APD
Responsivity (A/W)	Res	0,9	0,8
TIA noise density ($A/\sqrt{Hz}$)	σ_t	10^{-11}	$4\ 10^{-11}$
Multiplication factor	M	20	8
Excess noise factor	F	5	5

The model can be expressed in number of average photons in a *signal* slot or in function of received power by using the following correspondence: $n_s = \frac{\eta}{h\nu} P_s T_s$, where P_s is the peak received power ($P_s/2$ is the average received power) (W), $\eta = h\nu R_{res}/q$ is the quantum efficiency, $h\nu$ is the photon energy (J), $R_{res} = 0.9$ A/W is the APD responsivity.

The Custom APD parameters corresponds to an APD that has been characterized in the lab by ADS, it will be used in the latter part of the article to perform the simulations. If not specified, the CCSDS parameters are used.

3. COMMUNICATION CHAIN

The studied communication chain is composed of channel coding, channel interleaving, pseudo-randomization combined with repetition, frame synchronization, and in-band signaling.

3.1 Channel coding

When looking for candidate forward error correction (FEC) codes for optical communications, existing codes used for radiofrequency space communications were analyzed. Many of them, such as DVB-S2, SCCC, and ARJA/C2 LDPC codes, are performant and very close to the capacity, however they were designed for lower data rate, and at 10 Gbps the hardware complexity for both the encoder and the decoder become too high. Consequently, ADS with support of CNES has developed a new FEC technology for multi-gigabit optical communication downlinks. The goal was to achieve best signal

processing performances at a lower cost, in particular for the on-board side in which embedded constraints due to space environment are very demanding.

ADS has designed a new family of LDPC codes detailed in [7]. The LDPC family defines ARA- LDPC for high rates: 3/4, 4/5, 5/6, 7/8, 9/10, and Protograph-Based Raptor-Like LDPC Codes (PBRL codes) for low rates: 3/10, 3/8, 2/5, 1/2, 3/5, 2/3 with very good performances close to the Shannon limit.

An IP was developed, and it exhibits very good complexity figures. For a data rate of 10 Gbps, the encoder uses less than 3% of a space FPGA KU-60 (LUTs - few BRAMs), assuming strong derating (50%) on fMAX (200 MHz). The encoder has been optimized to increase the throughput/area of LDPC using Cascaded Partial-parallel architecture. One IP can handle several code rate in order to allow variable coding rate during a pass. The decoder uses less than 70 % of VUP-9 assuming strong derating (50%) on fMAX (250 MHz), it can be easily achieved on several high-end FPGA technologies (Xilinx, Intel). The throughput is guaranteed for all rates using an early termination scheme suitable for a very low floor below a BER < 10^{-12} .

Coding Efficiency	Very Good (close to capacity)/ no floor
Data Rate Scalability	High Suitable for 10 Gbps and more
Multi code Rate Scalability VCM/ACM ready	High very low complexity One IP core to support several code rates
Encoder Complexity CR = ½, 10 Gbit/s @ fMAX KU-60 -1	1.3% LUT6 <1% FF 1.6% BRAM36
Decoder Complexity CR = ½, 10 Gbit/s @ fMAX VU9P -2	42.3% LUT6 19.475% FF 55.6 Mbits BRAM/URAM

Rate	**Code type**	**Payload Size (k)**	**Punctured Size (N)**
9/10	ARA	27648	30720
7/8	ARA	26880	30720
5/6	ARA	25600	30720
4/5	ARA	24576	30720
3/4	ARA	23040	30720
2/3	PBRL	20480	30720
3/5	PBRL	18432	30720
1/2	PBRL	15360	30720
2/5	PBRL	12288	30720
3/8	PBRL	11520	30720
3/10	PBRL	9216	30720

The simulated bit error rate (BER) decoding performances for an AWGN channel is given in Figure 3 left. It corresponds to a case where the thermal noise is dominant. The Frame error rate using the CCSDS APD receiver model with thermal and shot noise is shown in Figure 3 right. The codes are close to capacity as shown in Figure 4. The new designed FEC responds effectively to the criteria of good performance and reduced complexity at high data rate.

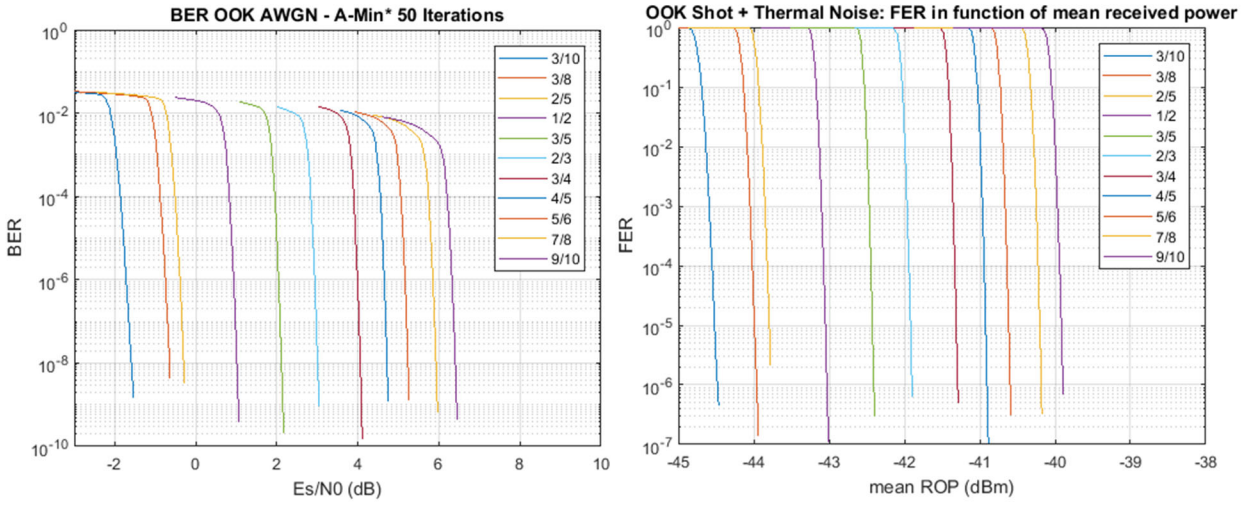

Figure 3: Bit Error rate in an AWGN channel (left), and frame error rate using CCSDS receiver model (right), both with A-Min* decoder

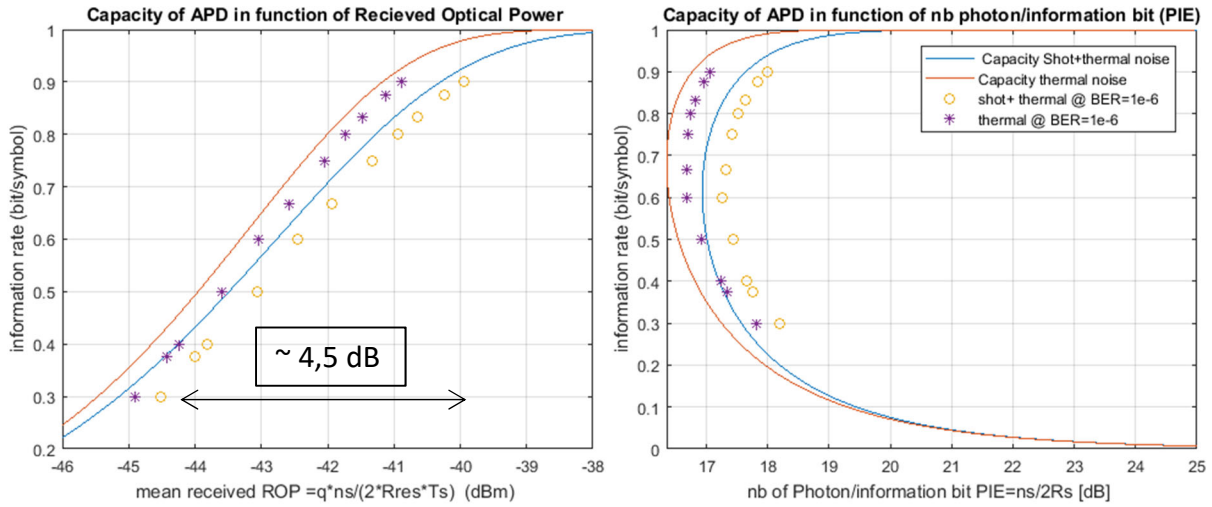

Figure 4: distance to capacity of the LDPC family in function of the mean received power (left), and in function of the number of photon per information bit (right)

3.2 Channel interleaver

In order to handle the varying optical transmission channel with fadings which coherence time is long compared to the code word length, the channel coder is paired with a long channel interleaver, that will introduce temporal diversity by interleaving multiple code words over several hundreds of milliseconds. For space communications, the convolutional interleaver is often used as it minimizes the required memory and latency. In case of optical communications the realtime constrains are high as the interleaver shall work at 10 Gbps, with the cumulated speed in write and read of 20 Gbit/s. On le the receiver side, the de-interleaver cumulated speed is 20 GByte/s in order to store the LLR used for soft decoding. Moreover, due to the need of long interleaving time, large memory is required, much larger than the available internal memory of in chip or FPGA, which imply the use of external memory. External memory have constraints: the memory access is multiple of octet and not bit, and due to memory access latencies, it is needed to transfer burst of data to reach the desired throughput. In addition to the mitigation of the turbulences impairments, the interleaving scheme needs to be compatible with variable coding and variable data rate methods. For all this reasons the proposed interleaving process is based on a row/column block interleaver.

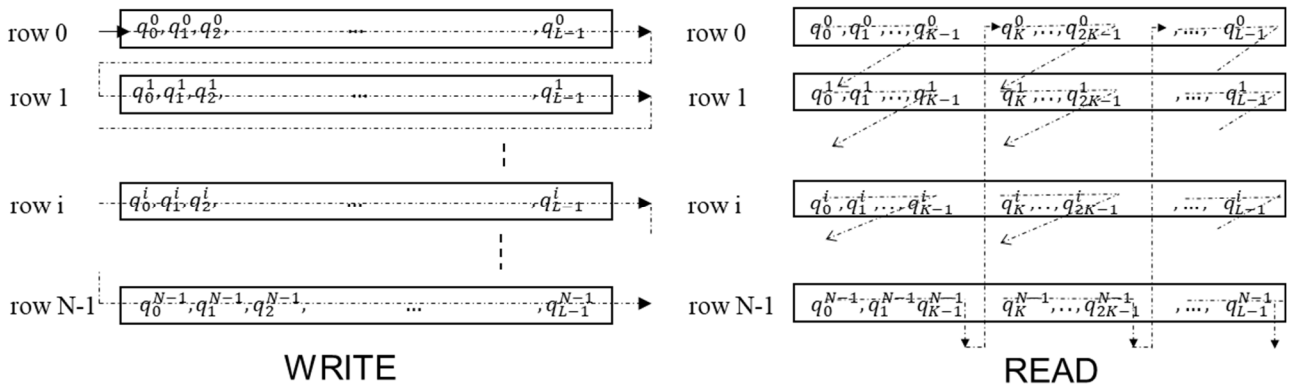

Figure 5: row/column block interleaver

Each codeword $\boldsymbol{q}^i$, composed of length L=30720 bits, $\boldsymbol{q}^i = q_0^i, q_1^i, \ldots, q_{L-1}^i$ is written row-wise in the interleaver, and the output is obtained by reading the interleaver column-wise by blocks of length K . The interleaver is parameterized with two parameters: K, the number of binary digits per interleaver symbol; and N, the number of rows in the channel interleaver, which are signaled by inline communication.

3.3 Performance assessment using bit by bit simulation

The performance validation of the proposed FEC and row/column block interleaver was assessed by simulation. The simulated chain is presented in Figure 6, and the input parameters given in Table 1. The simulator outputs per code words the BER, the FER, the mutual information and the received optical power (ROP).

Figure 6: bit by bit simulator

Table 1. simulation parameters

FEC	FEC Rate	LDPC R = 1/2
	Nb Iterations	25
	Implementation	OMS
Interleaving	Row/column interleaver time	50 ms, 500 ms
	Convolutional interleaver time	100ms then truncated to 50ms
	K (nb of bit per interleaver symbol)	128
Receiver model	Modulation / bit Rate	OOK, 10Gbps
	Optical detector type	APD custom model
Fading time series	Power vector	A and H
	Duration	100s

The FER are plotted in function of the static ROP in Figure 7 left. The first result is that the row/colum block interleaver exhibits similar performances compared to convolutional interleaver as expected. It is visible for vector A with integration time of 50ms. For vector H, at 50ms integration time neither the row/column nor the convolutional are sufficiently long to allow the convergence of the error correcting code, which means that in this configuration error free transmission cannot be done in the range of received power that was considered.

The degradations caused by the fading vectors and the finite length interleavers can also be seen in Figure 7 left. The loss compared to the case without fading is about 1 dB for vector A with interleaving time of 50ms, and about 4dB for vector H with interleaving time of 500ms. These values are in coherence with the difference between the static and ergodic capacity for vector H shown in Figure 7 right. The static capacity indicates the theoretical achievable performance assuming perfect error correcting codes of infinite length, and the ergodic capacity indicates the theoretical achievable performance under fading assuming perfect interleavers with infinite length. Without fading vector, the LDPC ½ has a 0.5 dB penalty compared to the static capacity, and due to the limited length of the interleaver, the result of simulation for the interleaved code words under fading vector H are 2 dB worse than the ergodic capacity. The distance to the ergodic capacity can be reduced by increasing the interleaving time, however from an implementation point of view, defining very long interleavers has a strong impact on the needed memory, especially at 10 Gbps. A compromise has to be taken between the loss implied by the reduced interleaving time, and the needed memory on-board the spacecraft, but also at the receiver ground station, as in the latter case the symbols are coded on several bits to allow soft decoding.

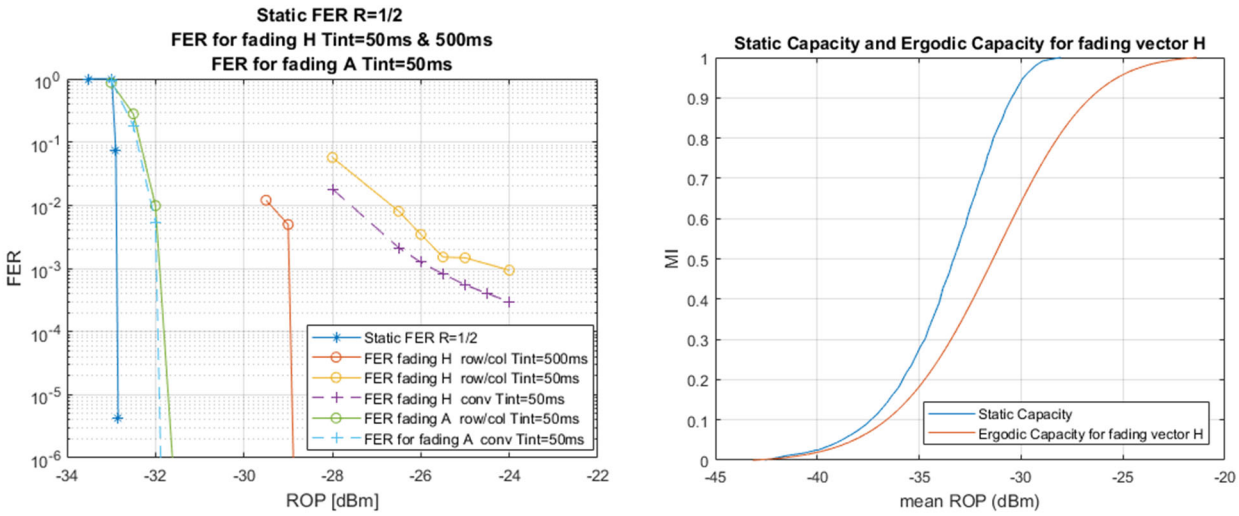

Figure 7: simulated FER with fading vectors and interleavers (left), static capacity and ergodic capacity for vector H (right)

3.4 Variable data rate

In space to ground transmissions using radiofrequency, Variable Coded Modulation (VCM) [8] defines the adaptation to the dynamic link by changing modulations and code rates. It defines how to rapidly switch the emitter configuration during a communications session to match dynamic link conditions in near real time. A similar approach has been proposed for optical communications. Indeed, dynamic conditions on the optical links also arise because of changes in geometry, weather, and atmospheric turbulence, as it was introduced in chapter 2. By adapting the transmitted signal to the link condition, the excess margin can be reduced and the total data throughput increased.
For optical communications, the adaptation can be made by using several techniques, the two selected in the defined communication chain are: variable code rate and variable repetition rate.

a. variable code rate

The defined family of LDPC range from rate 3/10 to 9/10 which provides several coding gain. For an OOK modulation and a receiver type APD, it can be seen in Figure 4 that between the maximum code rate and the minimum code rate, there is a dynamics of 4.5 dB that can be covered. This value increases to about 6.5 dB for receiver of type preamplied intensity modulation direct detection (IM-DD), as shown in Figure 8 left, with the capacity of OOK and DPSK in presence of a predominant ASE noise. The dynamic covered by the family of LDPC codes goes up to 8 dB for a BPSK coherent receiver, as shown in Figure 8 right, which make this family of codes an interesting solution for coherent transmissions. If the coding gain provided by the variable code rate is not sufficient to cover the dynamic range of the link, the complementary variable repetition rate scheme can be used.

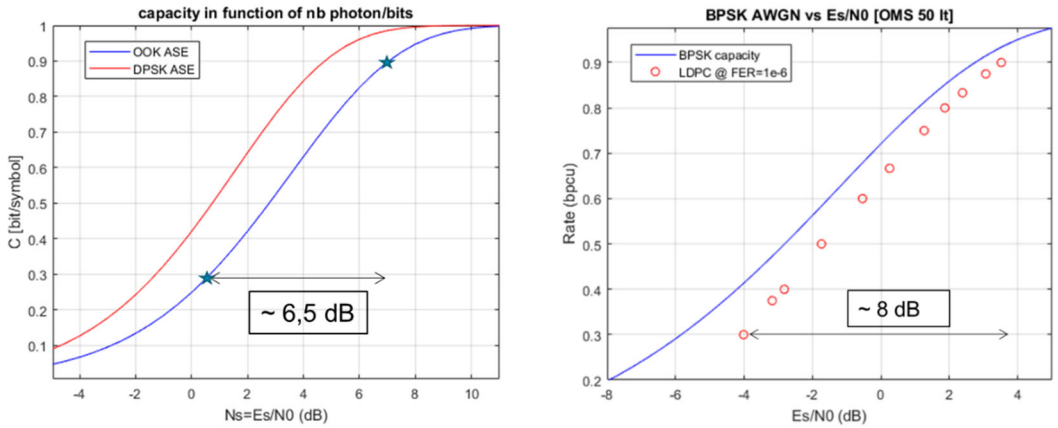

Figure 8: coding gain of the LDPC family for preamplified IM-DD receiver (left), and BPSK coherent receiver (right)

b. variable repetition rate

The variable repetition rate, also called variable data rate (VDR), was proposed by ESA [9] . The advantage of this technique is to be able to change the data rate on the fly and keeping the same optical front-end (APD + TIA) at the reception. Indeed with the proposed scheme, it is not needed to adapt the receiver bandwidth to the data rate. The principle is to increase the duration of a bit by repeating it several times and by multiplying them with a pseudorandom sequence. At the receiving end, the receiver optical front-end is optimized to receive the maximum symbol rate, and the received symbols are correlated with the sequence in the digital domain to obtain the transmitted bit. The implementation that is done in the actual communication chain varies compared to the initial proposal, especially for the signalization of the repetition rate and the choice of the pseudo randomizer to scramble the bits.

The simulation results can be seen in Figure 9, for a scenario without turbulence and using the APD custom receiver model. The frame error rate is given (left figure) for the code rates of the LDPC family 3/10, 1/2, 2/3, 4/5 and 9/10, and for code rate 3/10 using the repetition rate of 2, 4, 8, 16 and 32. By dividing by 2 the data rate, it is possible to gain 1.5 dB of power. The variable repetition allows in this example to receive a signal more than 7 dB weaker for the repetition rate 32 compared to the code rate 3/10 without repetition. But it is at the cost of the useful data rate as it can be seen in the figure on the right, which represents the power gain compared to a non-coded case fir the LDPC family and the code of rate 3/10 with repetitions. Using repetitions allows to transmit on a link that has strong attenuations, but the total volume of data that can be transmitted during a pass will not increase dramatically when the larger repetition rate are used.

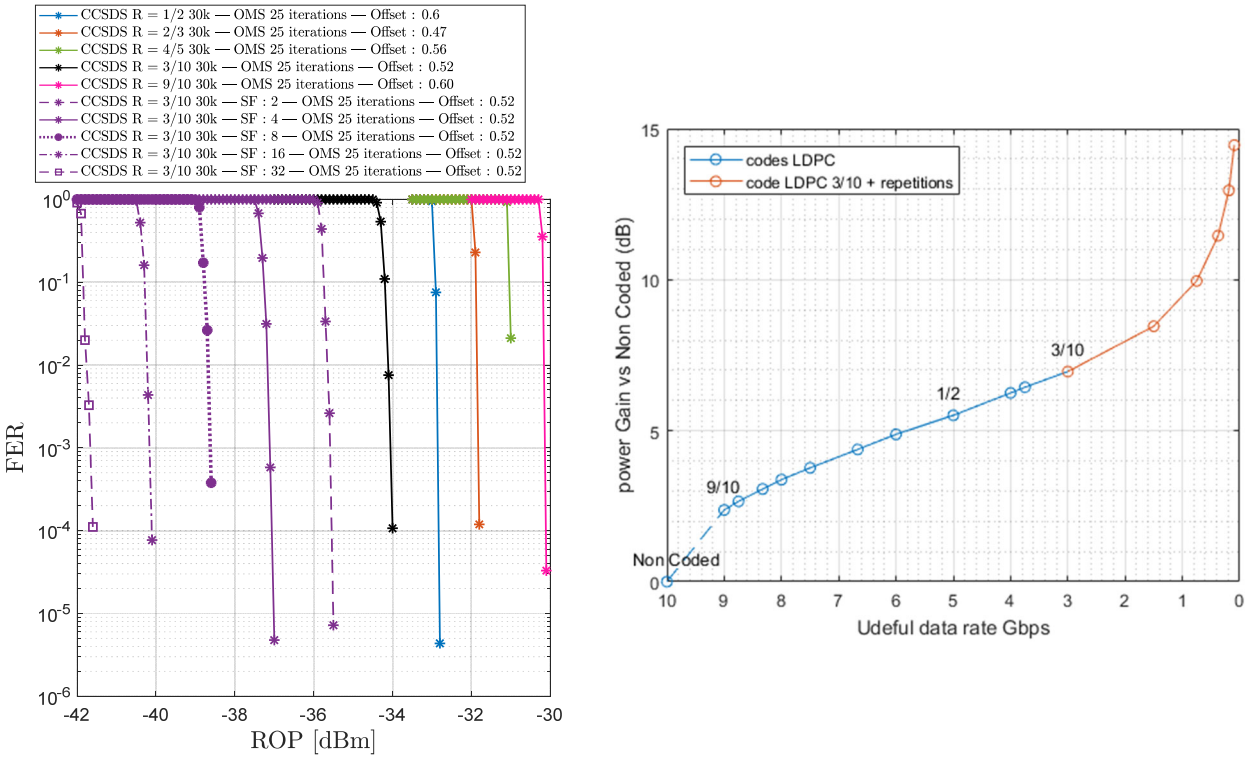

Figure 9: simulated FER for LDPC of rates 3/10, 1/2, 2/3, 4/5, 9/10 and code rate 3/10 with repetition rate of 2, 4, 8, 16, 32(left); power gain compared to non-coded obtained using variable repetition rate in function of the useful data rate, for a symbol rate of 10 Gbps (right)

3.5 Synchronization layer framing

A framing structure was defined, that relies on the philosophy used for DVB-S2. It includes in-band signaling and robust detection and synchronization on the optical transmission channel. The in-band signaling field allows to select the code rate and the repetition rate dynamically during a pass according to the elevation of the satellite.
A synchronization layer frame is composed of all the LDPC code words that are interleaved in the row/column block interleaver, repeated and scrambled. Its length depends on the interleaving time and the repetition rate. The frame starts by a synchronization marker followed by the inband-signaling field. It is possible to add intermediate synchronization marker and inband signaling fields within the frame at fixed interval. The distance between 2 synchronization markers is parameterized in order to let the system designer choose between a robust synchronization with very short reacquisition time but an increased overhead, or a less robust synchronization with very low overhead.
Both the synchronization marker and the in-band signaling fields are based on gold sequences of length 2048 bits. The Gold code generator that was selected corresponds to the real part of non-coherent return PN standardized in section 5.3 of [10]

a. Frame synchronization marker

The frame synchronization marker is a gold sequence of length 2048, that is repeated at the beginning of each frame and within the frame at parameterized fixed distance. A number of analysis have been performed to assess the synchronization performance in function of the time between each synchronization markers and in function of the number of bits used for the detection. Indeed, in order to reduce the complexity of the receiver it is possible to perform a correlation on a truncated part of the marker like 512 or 1024 instead of the whole 2048 bits. An example of analysis is shown in Figure 10 , with the following assumptions: APD custom model, no turbulence, truncated correlation on 512 bits, distance between synchronization headers equals to 16 times the length of a codeword (30720), which corresponds to a time between headers of 50µsec, and an overhead due to signaling < 1%. Figure 10 presents the probability of false alarm and the probability of miss detection assuming a blind search of the synchronization marker. The threshold of the correlation process is chosen by the system designer in function of the desired probability of false alarm. The probability of miss detection is function of the received power. The curve of miss-detection on the right was simulated with a threshold computed based on a false alarm probability of 10^{-2}. This example shows that with a correlation on 512 bits, and a blind search algorithm , the detection is good for a received power down to -37 dBm. Which means, by looking at Figure 9, that it is not suitable for transmission of code rate 3/10 and repetition rate superior to 2 that are received with a lower power. This is the reason why the synchronization marker is long (2048), it was defined in order to allow synchronization at low power when high repetition rate is used.

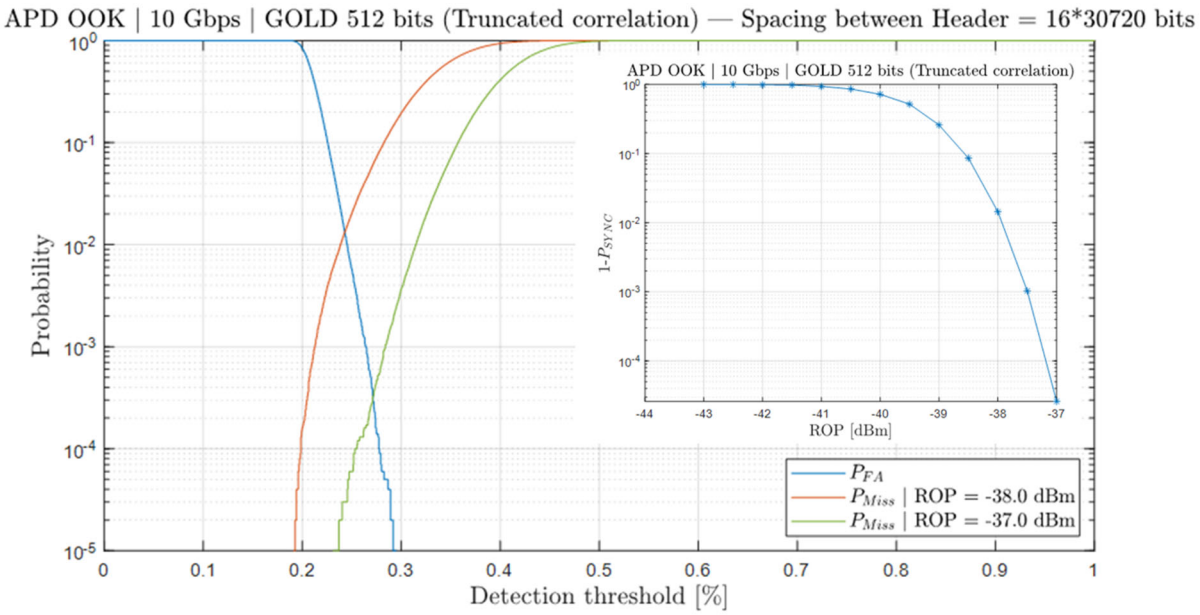

Figure 10: probability of false alarm and probability of miss-detection of the synchronization marker

b. Inband signaling

In-band signaling is a method to communicate dynamically changing signal parameter values to the receiving end, using the communications link itself. The in-band signaling can be detected at the receiving end, which allows the receiver to recover the parameter values and properly configure itself to receive the remainder of the transmission. The in-band signaling is accomplished with a frame signaling field, that comprises 2048 bits that contains the Mode ID, which identifies the Emitter configuration to be used to properly receive the Frame. This field is generated using the same Gold codes than for the synchronization marker.

The emitter configuration is defined as a set of parameters that can change dynamically during a mission phase and which values are to be sent to the receiver. These parameters are listed in an emitter configuration table. In the defined communication chain, the parameters that can changedynamically are the code rate, the repeat factor, and the channel interleaver length. An example of emitter configuration table is given in Table 2, where during a pass it will possible to switch between 6 different modes, identified by a mode ID, ranging from a code with rate 9/10 to a code of rate 1/2 and repetition rate of 16.

Table 2. example of emitter configuration table

Mode ID	Code rate r	Repeat factor	Number of rows in the interleaver
0	1/2	16	8192 (65536/8)
1	1/2	8	16384 (65536/4)
2	1/2	4	16384 (65536/4)
3	1/2	2	65536
4	1/2	1	65536
61	9/10	1	65536

The performances of the in-band signalization field detection have been assessed by simulation. Some results are presented in Figure 11, on the left the probability of bad selection of the mode ID among 8 possible emitter configurations, in function of the received power for correlation on 512, 1024 and 2048 bits. The figure on the right illustrates the penalty when searching for a mode ID among 32 possibilities instead of 8. At high probability of success, the penalty is moderated, in the order of 0.5 dB, and at probability of 10^{-1} it is about 1dB.

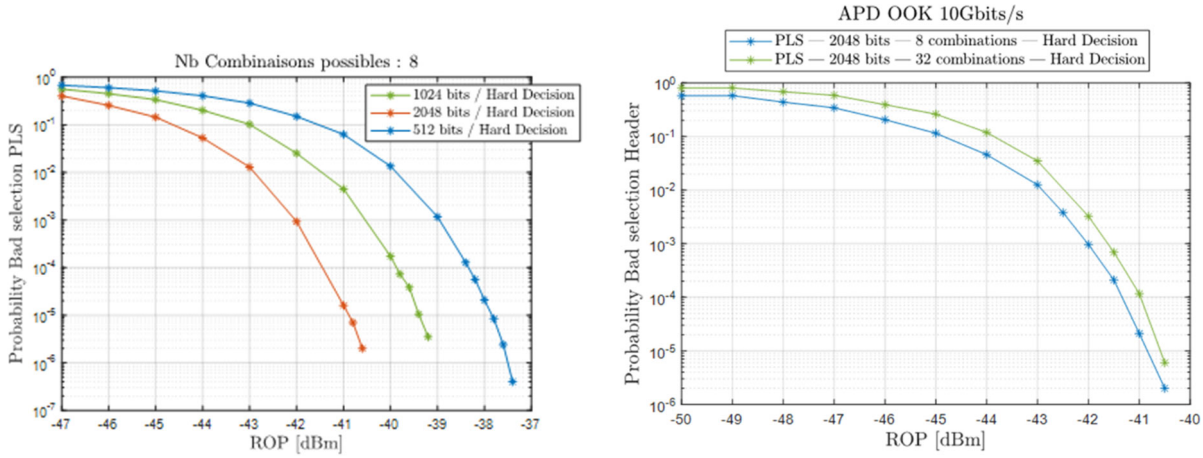

Figure 11: probability of bad selection of mode ID (left), probability when searching the mode ID among 8 or 32 possible combinations (right)

4. LAB MEASUREMENTS

The previous chapter presented the communication chain and its validation using simulations. The communication chain has been implemented on representative flight hardware and ground station receiver hardware and its performances are currently under validation in the optical laboratory of airbus defence and space in Toulouse. The bench is composed, on the emitter side by the electronic board (TCE) in charge of the channel coding and interleaving, repetition, scrambling, and framing, the photonic board (LCE) that perform the OOK modulation, and the power amplifier (LPE). The optical channel emulator is composed of 2 variable optical attenuators, including a high speed attenuator to apply fading time series. On the receiver side, the optical front end is composed of an avalanche photodiode that is connected to a digital receiver (ODPU) that is in charge of the analog-to-digital conversion of the signal, the synchronization, the de-spreading, de-interleaving and LDPC soft decoding. The complete chain is working in real time at 10 Gbps.

The test bench has already been validated for a 10 Gbps DPSK pre-amplified chain for the demonstrator TELEO [11], and it is currently set-up for LEO DTE. Figure 13 illustrates the preliminary tests that were made to select the appropriate RF amplifier to install in the cortex lasercom of safran data system. Indeed, the RF level at the output of the APD being low, it is needed to amplify it before the digital processing. The BER before decoding are presented in the right figure for 2 RF amplifier configurations, and compared to the BER corresponding to the Gaussian model of the APD. The lab measurements slopes differ from APD noise model at high SNR, it may be explained by the effect of other noise contributors such as RF amplifier and ADC quantification noise. When FEC will be used the difference should be reduced.

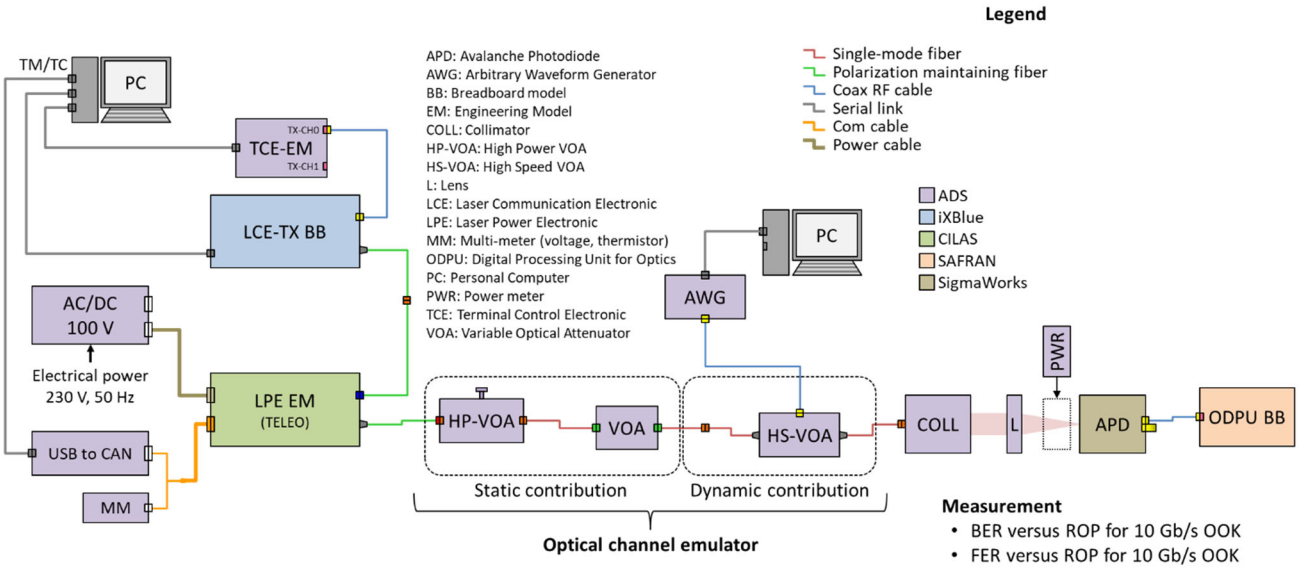

Figure 12: End to end LEO DTE test bench at ADS Toulouse

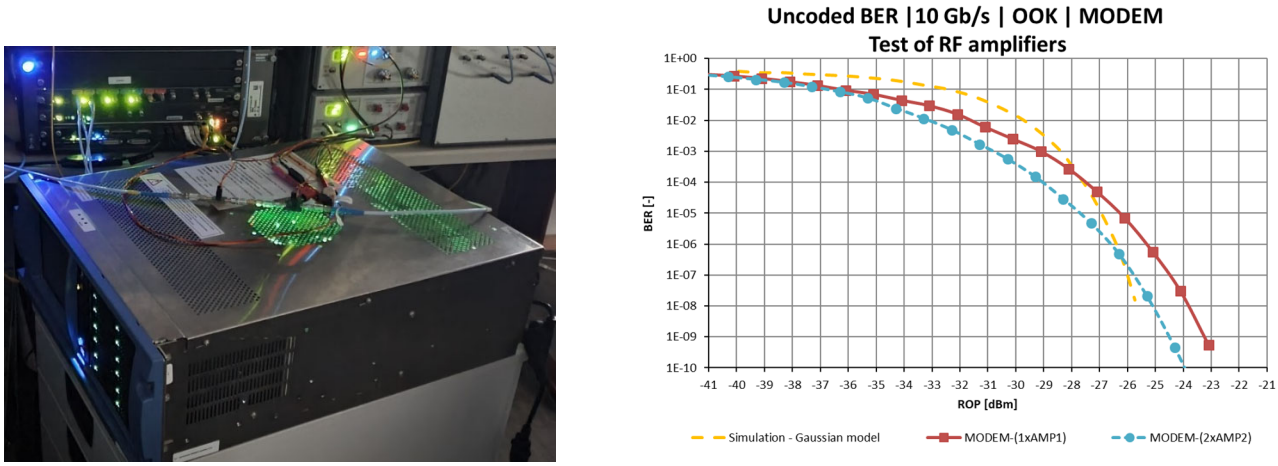

Figure 13: The digital receiver cortex Lasercom and tested input RF amplifiers (left), BER for 3 configurations (right)

5. IN-ORBIT DEMONSTRATION

Airbus Defence and Space and CNES are planning two demonstrations: a GEO feeder link demonstration [11], and a LEO DTE demonstration [12]. The communication chain of the 2 demonstrations share many communalities: on the downlink part, the 2 demonstrations will use the defined LDPC codes, row/column block interleaver, repetition rate, and a similar synchronization layer framing structure with synchronization marker and in-band signaling. It will be tested in real condition with two modulations: DPSK for the GEO demonstration (2023) and OOK for the LEO demonstration (2024).

6. CONCLUSION

ADS with support of CNES has developed a cost-efficient and flexible modem technology for multi-gigabit optical communication downlinks. To tackle this challenge, the synchronization and channel coding sublayer of the optical waveform has been designed to achieve best signal performances by taking into account hardware constraints of state-of-the-art on-board and ground hardware data processing technologies. This new coding and synchronization layer for space optical communication, has been designed to be flexible in order to adapt to a variety of link conditions, modulations, and receiver architectures. The results have been presented, in this article, for the case LEO DTE OOK with an APD receiver that corresponds to the use case of the newly standardized CCSDS O3K. Similar validations by simulation and end-to-end test on laboratory bench in real time have been done for a preamplified DPSK receiver, and will be done for a preamplified OOK receiver. This new communication chain will be demonstrated in orbit on a GEO mission and a LEO mission during 2023 and 2024.

ACKNOWLEDGMENTS

The main author would like to thank Raphaël Le Bidan from IMT Atlantique for his expertise in information theory and in particular for the formulation of the static and ergodic capacities for different type of receiver.

REFERENCES

[1] https://cwe.ccsds.org/sls/default.aspx#_SLS-OPT, pinksheet OPTICAL COMMUNICATIONS CODING AND SYNCHRONIZATION, RECOMMENDED STANDARD CCSDS 142.0-B-1
[2] B.S. Robinson, C.M. Schieler, D.M. Boroson, "Large-Volume Data Delivery from Low-Earth Orbit to Ground Using Effcient Single-Mode Optical Receivers", SPIE LASE 15 March 2016
[3] D. Giggenbach & al, "Reference Power Vectors for the Optical LEO Downlink Channel", ICSOS 2019
[4] Dirk Giggenbach, Amita Shrestha , "O3K: Reference Optical Downlink Power Vectors v20191205", CCSDS SLS-OPT
[5] D. Giggenbach, R. Mata-Calvo, "Sensitivity Modeling of Binary Optical Receivers", Applied Optics, Vol. 54, No. 28, pp 8254-8259 / October 1, 2015
[6] Jon Hamkins and Dariush Divsalar,CCSDS Optical Communications Working Group, monthly meeting, April 14, 2020
[7] Benjamin Gadat, Lyonel Barthe, Balazs Matuz, Charly Poulliat, "LDPC Codes with Low Error Floors and Efficient Encoders", to be published.
[8] *Variable Coded Modulation Protocol.* Issue 1. Recommendation for Space Data System Standards (Blue Book), CCSDS 431.1-B-1. Washington, D.C.: CCSDS, February 2021.
[9] Pantelis-Daniel Arapoglou, Nicolò Mazzali, "System-level benefit of variable data rate in optical LEO direct-to-earth links," Proc. SPIE 11852, International Conference on Space Optics — ICSO 2020,
[10] Data Transmission and PN Ranging for 2 GHz CDMA Link via Data Relay Satellite. Issue 1. Recommendation for Space Data System Standards (Blue Book), CCSDS 414.1-B-1. Washington, D.C.: CCSDS, September 2011
[11] Poulenard, S., "10 Gbauds digital optical bidirectional link performances between an optical ground station and a geostationary satellite", ICSO 2022
[12] Lochard J., de Guembecker N., "LASIN optical link on-board CO3D constellation" , ICSO 2022